The Effect of Microcirculation Disturbance of Peribiliary Vascular Plexus on Hepatic Bile Duct Epithelial Cells in Rats Undergoing Liver Transplantation and Postoperative Rejection Reduction by Nanocarrier Mediation

Zhigao Yuan, Mai Zhou*, Wuyi Deng, Daqing Wang, Gangjun Jiao

Department of General Surgery, Civil Aviation General Hospital, Beijing, 100123, China

ARTICLE INFO

ABSTRACT

This study was to investigate the effect of microcirculation disturbance of PVP on HBD epithelial cells in rats undergoing liver transplantation and to explore the postoperative rejection reduction by nanocarriers mediation. For this aim, adult male rats weighing 210–250 g, were fed cleanly and were subjected to liver transplantation. 3 days after the surgery, the rats were randomly divided into three groups based on different intervention factors: group A (HAL), group B (HAMI combined with HAL), and group C (control). The three groups of rats were divided into three subgroups according to the duration of the University of Wisconsin (UW) solution (UW time) used to preserve the donor organs for transplantation, which were 2h, 8h, and 16h, respectively. In addition, the RNA sequence of rat class-II transactivator (CIITA) the rat was searched, and the target interference sequence was designed concerning the RNA. Results showed that the carrier nanoparticles were spherical without obvious oxygen vacancies, the distribution was relatively tight and concentrated, and the main particle size was 50-140 nm. As the mass ratio of HGPAE to DNA increased, the mobility speed of the nanocarrier/shRNA plasmid complex decreased due to the decrease in surface charge. When the mass ratio reached 90:1, the mobility of the complex was completely blocked, suggesting that the DNA was completely compounded. The counts of PCNA, CK-19, F-VIII-Ag, VEGFA, VEGFB, and VEGFC in the 3 groups all showed a downward trend with the increase of UW time; the count in group B was lower than that of groups A and C. In the PCNA count statistics, there was no obvious difference between group A and group B at UW8h, but there were differences in contrast to group C ($p<0.05$). It was concluded that the blood supply of the microcirculation of the PVP was extremely important for the transplanted liver tissue. When the blood vessels around the HBD of the rat were completely ischemic, the HBD epithelial cells became the most important target of damage, and the proliferation and changes of the HBD epithelial cells can be directly observed. In addition, the nanocarrier-mediated genes were applied to discuss postoperative rejection. The expression of class-II MHC-II gene in nanocarrier CIITA-shRNA was inhibited, which interfered with the recipient's immune recognition of the graft, thereby reducing the intensity of the rejection reaction and relieving the rejection reaction.

Introduction

Liver transplantation is the only effective treatment for end-stage liver disease. Patients who can't be cured with conservative treatment and may die within 6 - 12 months are recommended to be treated with liver transplantation (1). The first case of liver transplantation in China was in Shanghai in 1977. After decades of development, liver transplantation has become the most effective treatment for end-stage liver disease. However, according to relevant research reports, the long-term survival rate of patients after liver transplantation is not high in China, the incidence of postoperative HBD complications is still 6.1-25.3%, and the mortality rate caused by HBD complications is still as high as 13.1%. Therefore, the treatment of HBD complications is of important significance for the long-term survival rate of patients after liver transplantation (2).

Current studies have shown that the occurrence of HBD complications may be related to blood-type HBD damage. The blood supply of HBD mainly comes from the hepatic artery. The distribution veins at the end of the hepatic artery and the portal vein can be divided into smaller capillaries, which are

*Corresponding author. E-mail: yuan_zhigao2021@163.com

connected with sinusoids (3). The epithelial cells of HBD cover the intrahepatic bile duct epithelium. In the related studies of cholestasis, it can be found that the vascular epithelial factor compensatory hyperplasia and the bile duct tissue is very susceptible to ischemia-reperfusion vascular injury (4). There are more and more studies on the influence of microcirculation on vascular epithelial cells in recent years, and it can be inferred that microcirculation disturbance will have a continuous impact on vascular epithelial cells. In this study, the effect of intrahepatic microcirculation disturbance of PVP on epithelial cells after liver transplantation was studied based on the establishment of an animal model of liver transplantation in rats (5).

Rejection is a major problem faced by allogeneic liver transplantation. The time or severity of rejection is clinically divided into hyperacute rejection, acute rejection, and chronic rejection (6). The type of cells attacked, pathologically, can be divided into cellular rejection and humoral immune rejection. Hyperacute rejection refers to the presence of antibodies against the donor in the patient before transplantation. When the liver receives the open blood flow in the patient's body and comes into contact with the recipient's blood, the pre-existing antibodies regard the liver as an antigen, so the antigen-antibody appears, which activates the coagulation factor in the cell, so that combined liver quickly develops thrombus from small blood vessel to large blood vessel. After the blood supply is stopped, the color of the connected organ changes, and then the function is lost until the organ is necrotic (7). Acute rejection usually occurs within a few days to a few weeks after surgery and can be manifested as fever, fatigue, elevated transaminases, and elevated bilirubin. Its diagnostic criteria require pathological examination, and the changes in liver structure can be observed under a microscope (8). Chronic rejection usually takes a few months or a few years after surgery, so its damage process is slow and difficult to find. At present, the cause is not fully clear. The main clinical manifestations are vasculitis, vascular fibrosis, occlusion of small arteries, and gradual loss of function of organs (9). Severe rejection can lead to the loss of function of the transplanted organ, requiring another transplant. Therefore, reducing postoperative rejection is very important, which has to be solved urgently in clinical practice

(10). Gene therapy plays a key role in the study of rejection after liver transplantation (11). In this study, a nanocarrier-mediated gene model was adopted to study the rejection after transplantation. The β-amino ester in nanomaterials is a new type of cationic polymer, which has been used in the field of gene carriers due to its diversity, good biocompatibility, and biodegradability (12, 13). In this study, HGPAEs were applied to the rejection study of transplanted animal models. The results of the study were reported as follows.

Materials and methods
Experimental animals and grouping

Adult male rats (Experimental Animal Center of the Third Military Medical University) were selected, weighing 210 - 250 g, and they were cleanly fed. The donors and recipients fasted for 12 hours before surgery, but they can drink freely. The animals were kept in a constant temperature (20 ± 1.2°C) and constant humidity (57 ± 3%) laboratory. All experimental procedures were carried out in accordance with the ethical principles of animal experiments.

Liver transplantation was performed on the rats. 3 days after the transplantation, the rats were randomly divided into three groups and were given different intervention factors: Group A (HAL), Group B (HAMI combined with HAL), and group C (control group). The three groups of rats were rolled into three subgroups according to the UW time used to preserve the donor organs, which were 2h, 8h, and 16h in sequence.

Methods for surgery and specimen preparation

Firstly, the donor rats were weighed and then taken the supine position after anesthesia. The limbs were fixed, the upper abdominal transverse incision was made, the excess tissue was stripped, the liver was completely exposed, and then injected with Ringer's solution (4°C) into the surface to cool down. After the liver tissue became evenly white, it could start to free the liver, cut the vein, separate the common bile duct, and perform ligation. After the donor liver was removed, it was stored in a preservation solution at 4°C. The preservation time was UW2h, UW8h, and UW16h. Then, the liver tissue of the recipient was excised, and a small amount of liver tissue was needed

to keep the vena cava severed open. After the liver was removed, the rat entered the anhepatic phase. The donor liver was taken out, and the surface was washed under Ringer's solution at 4°C. The upper and lower vena cava of the donor liver was matched with those of the recipient. After correctness, suture was performed to end the anhepatic period. The color of the right kidney of the rat was observed until it was recovered to normal. Next, the outer end of the internal stent of the common hepatic artery of the donor was inserted into the common hepatic artery of the recipient to suture the cut with No. 9 silk thread. The vascular clip was removed, the blood supply of the hepatic artery was opened, and the abdominal wall skin was sutured. After the surgery, the rat was placed in a cage alone, and 10% glucose solution was given freely to drink. After 24 hours, the rat was given a normal diet. 3 days after the first surgery, the second surgery was performed according to the requirement of different groups, and different intervention factors were given. The hepatic artery was ligated again after the surgery.

After the rat recovered to normal, the histopathological biopsy could be performed. The liver tissue fixed with 5% paraformaldehyde would be made into wax blocks and cut into 5 um sections, and the slides were prevented from falling off by microwave repair antigen staining procedures. The slices were treated with conventional deparaffinization to water, washed 3 times with distilled water, then immersed in a microwave oven in citrate buffer (0.02 M, PH 6.1) and heated to boiling. 10 minutes later, the above operations were repeated 2-3 times. Then, it was washed after cooling, added with 5% blocking solution, and stored at room temperature (22°C). After the excess liquid was removed, the diluted mouse primary antibody was dropped to keep overnight at 5°C. The biotinylated goat anti-mouse IgG was dropped, the slices were washed with phosphate-balanced saline for 6 minutes, lightly counter-stained with hematoxylin for 3 minutes, and then mounted after dehydration to observe under a microscope.

Preparation of nanocarrier shRNA plasmid of CIITA gene

The CIITA RNA sequence of the rat was searched, a targeted interference sequence was designed with reference to RNA, and a negative control sequence was designed to exclude the gene homology of the rat so as to obtain the targeted shRNA eukaryotic expression and control vector, which were identified by DNA sequencing.

Preparation of HGPAEs/shRNA plasmid complex

The nanocarrier HGPAEs (Nano Research Institute, School of Materials Science and Engineering, Tianjin University) were added to a pH 5.3 sodium acetate/acetic acid buffer solution to prepare a carrier solution with a concentration of 2mg/ml. The HGPAEs solution was combined with the DNA plasmid solution at different mass ratios for compounding, incubated at room temperature for 40 minutes, and then performed an agarose gel blocking experiment. HGPAEs encapsulated pDNA, forming the compact nanoparticles with concentrated electric charges. After the minimum binding ratio of HGPAEs to pDNA was determined, the morphology of the formed complex was characterized and observed with transmission electron microscopy (TEM). The gel electrophoresis diagram of the nanocarrier/shRNA plasmid complex was observed, and the method of which was described as follows. The rat liver tissue was placed in a homogenizer for homogenization, and the protein of the sample to be tested was standardized based on protein standards. Then, a 20% separation gel was prepared for protein separation. The separated protein was transferred to a polyvinylidene fluoride membrane, which was sealed, added with the primary antibody, kept at a constant temperature overnight, and then added with the secondary antibody. An appropriate amount of concentrated SDS-PAGE protein loading buffer was added to the prepared protein sample to reduce the sample volume. The solution was heated in a water bath at 100 °C for 3-5 minutes to fully denature the protein. After the protein sample was cooled to room temperature, the sample was loaded directly into the sample hole of the SDS-PAGE gel to observe the electrophoresis result.

Statistical methods

SPSS 22.0 statistical software was employed for data analysis. The count data was expressed as [case (%)], using t-test, and comparison among groups was indicated as ($\bar{x} \pm s$), using the χ^2 test. The survival rate was analyzed with the Kaplan-Meier method, and

$P < 0.05$ suggested that the difference was statistically meaningful.

Results and discussion
Characterization of nanocarrier

Figure 1 showed that the carrier nanoparticles were spherical without obvious oxygen vacancies, the distribution was relatively dense and concentrated, and the particle size was 50 - 140 nm.
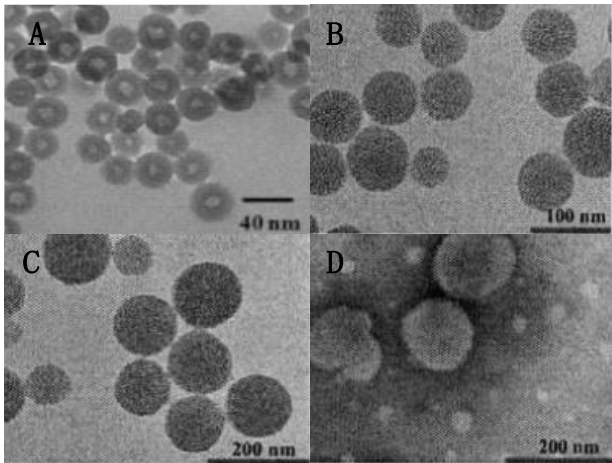

Figure 1. Characterization of the nanocarrier. Note: Figures A, B, C, and D showed the characterization of nanocarrier when the mass ratio of HGPAEs and DNA was 70:1, 80:1, 90:1, and 100:1, respectively.

Gel electrophoresis diagram of nanocarrier/shRNA plasmid complex

Figure 2 showed that as the mass ratio of HGPAEs to DNA increased, the mobility speed of the nanocarrier/shRNA plasmid complex decreased due to the decrease in surface charge. When the mass ratio reached 90:1, the mobility of the complex was completely blocked, indicating that the DNA was completely compounded.

Figure 2. Gel electrophoresis diagram of nanocarrier/shRNA plasmid complex.

PCNA

It was found that the PCNA counts of the three groups all showed a downward trend with the increase of UW time. The counts of group A and group B were much lower than the count in group C, while that in group B was the lowest. In addition, the counts in groups A and B at UW8h showed no obvious difference ($p > 0.05$), while showed great difference in contrast to other groups ($p < 0.05$), as illustrated in Figure 3.
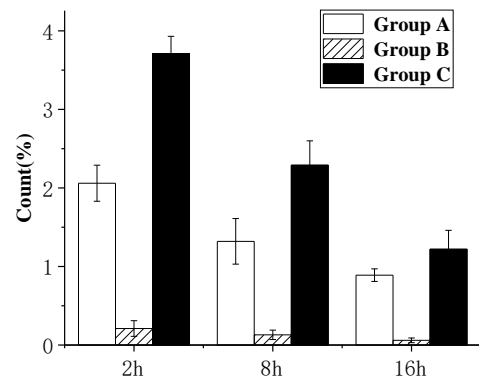

Figure 3. Count of PCNA.

CK-19

Figure 4 illustrated that the CK-19 counts of group C at 3-time points were higher in contrast to those of group A and group B and that group B was the lowest, showing statistical differences among the three groups ($p < 0.05$).
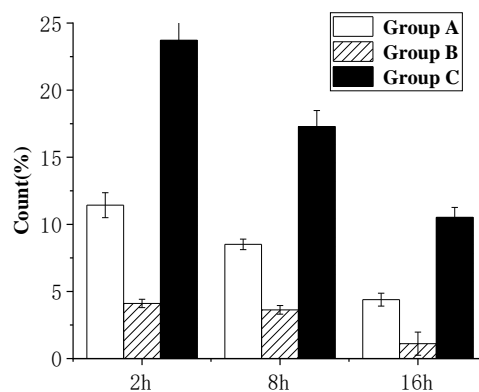

Figure 4. Count of CK-19.

F-VIII-Ag

As revealed in Figure 5 below, the counts of F-VIII-Ag in the three groups all showed a downward trend with the increase of UW time. The counts in group A and group B were observably lower than

those of group C, and those in group B were the lowest, showing remarkable differences among the three groups (p < 0.05).
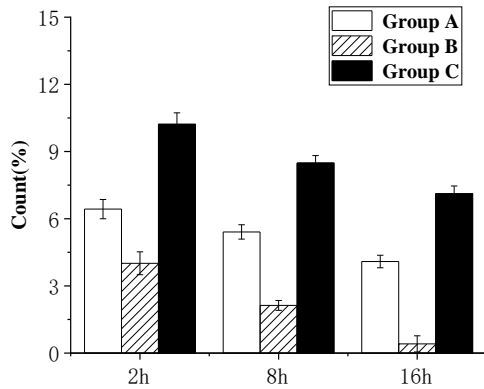

Figure 5. Count of F-VIII-Ag.

VEGFA

Statistics found that the VEGFA counts in all groups showed a downward trend with the increase of UW time. As given in Figure 6 below, the counts of group A and group B were lower greatly than those of group C, and those in group B were the lowest. However, there was no statistical difference in the change of count within group C (p > 0.05), the differences among the three groups were statistically obvious (p < 0.05).
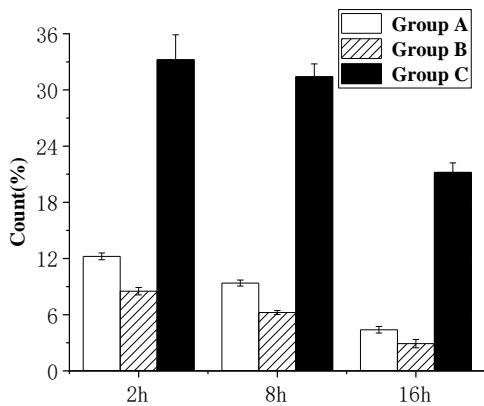

Figure 6. Count of VEGFA.

VEGFB

As illustrated in Figure 7, the VEGFB counts in group A and group B decreased with the increase of time at 3-time points; the count of group C was the highest at UW8h, the count of group B was the lowest at UW8h, and the difference was remarkable in statistics (p < 0.05).
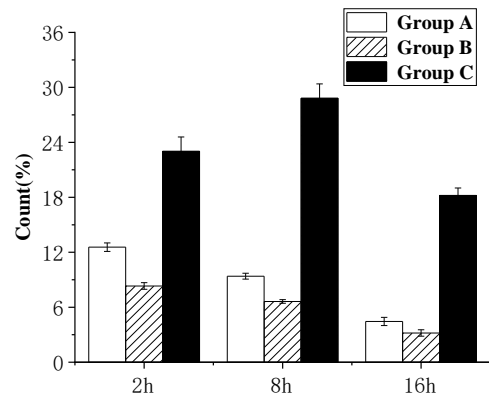

Figure 7. Count of VEGFB.

VEGFC

Figure 8 disclosed that the VEGFC counts of group A and group B decreased with the increase of time at 3-time points, but those in group C were the highest at UW8h, and those in group B were the lowest at UW8h. In addition, the differences were not statistically obvious among the three groups at UW16h (p > 0.05).
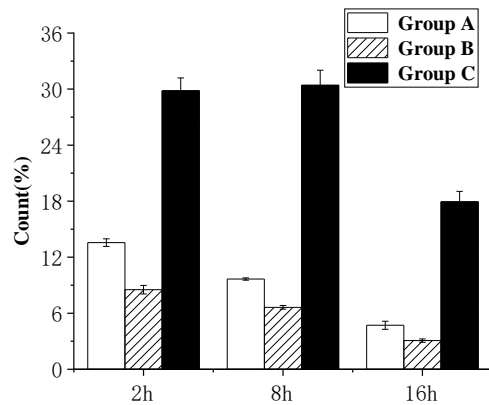

Figure 8. Count of VEGFC.

Anatomical studies have found that the blood supply of the HBD mainly depends on the blood flow of the hepatic artery, but recent studies have shown that in patients undergoing hepatic artery resection, the portal vein can also dominate protein breakdown, thereby protecting the structure and function of the HBD (14). In order to further confirm that the portal vein can control protein by reflux, the relevant researchers have reconstructed the liver blood flow in the portal vein after hepatectomy in rats and found that the levels of bilirubin and plasma protein in the rats were also within the normal range after hepatectomy, which proves that arterialization of the portal vein in rats is feasible. After the HBD of rat

loses the blood supply of the hepatic artery, the normal physiological function of the HBD can be guaranteed if the blood oxygen content of the portal vein reaches a compensable level. In this study, it was confirmed that excessive liver tissue ischemia could inhibit the damage of the HBD, and HAL alone was not enough to induce ischemia of the rat HBD (15).

In group B (HAMI combined with HAL) in this study, the lack of hepatic artery blood supply caused severe damage to the liver tissue and intrahepatic bile duct, which had a serious impact on the autocrine function of HBD epithelial cells, causing its cells count was lower than that of simply ligating the hepatic artery. The specific research results were that the counts of PCNA, CK-19, F-VIII-Ag, VEGFA, VEGFB, and VEGFC in the three groups all showed a downward trend with the increase of UW time, and the counts of group A and group B were obviously lower than those of group C, and those in group B was the lowest; there was no extreme difference in PCNA count between group A and group B at UW8h, and there was an obvious difference in contrast to other groups ($p < 0.05$). The results of this study were similar to the findings of related studies (16). In addition, related research reports have found that the lobular necrosis was visible in the slices of pathological tissues, and the mortality rate of rats showed an obvious increasing trend as time went by, which further showed that the blood supply of PVP microcirculation in the liver is extremely important for the transplanted liver tissue. When the blood vessels around the HBD of the rat are completely ischemic, the HBD epithelial cells become the most important target of injury, and the proliferation and changes of the HBD epithelial cells can be directly observed. VEGF can stimulate the formation and expression of new blood vessels to play a compensatory role in peripheral circulatory disorders and promote the repair of HBD epithelial cells (17, 18).

In addition, the nanocarrier mediation was adopted to reduce postoperative rejection, and the shRNA plasmids can be effectively delivered into target cells. It has the advantages of low toxicity, high efficiency, large capacity, and controllable gene transduction and expression, so it has become a research hotspot for the majority of researchers. As gene carriers, HGPAEs have the potential to compound negatively charged genes, promote gene escape from endosomes, and achieve gene release. In this study, nanocarrier/shRNA plasmid complexes were prepared and applied to couple with DNA. It was found the best mass ratio of HGPAEs to plasmid DNA was 90:1; it could compress the plasmid through electrostatic action and combine to form a nanocomposite with a particle size of 50 - 140 nm and a positive surface on the surface; it could bind to the plasmid DNA, forming stable nanocomposite, thereby providing effective protection to genes and the ability to release genes in acidic conditions. In this study, intraportal injection of nanocarrier plasmid complexes was adopted to transfect the liver to interfere with the donor liver and reduce the expression of related genes in the donor liver (19). Some researchers have found that the expression levels of CIITA and MHC-II genes in the nanocarrier CIITA-shRNA receptor show a decreasing trend, the rejection degree is also greatly reduced, and the survival time of the rat is prolonged obviously. Such results indicated that the method of silencing the expression of the CIITA gene of the donor graft can effectively suppress the rejection reaction and obtain a longer survival time. According to research reports, this mechanism may be due to the suppression of MHC-II gene expression in the nanocarrier CIITA-shRNA, which interferes with the immune recognition of the graft of the recipient, thereby reducing the intensity of the rejection reaction and further reducing the rejection reaction (20). In addition, CIITA can also participate in the regulation of the expression of a variety of antigen-presenting genes, which may also be partly involved in the outcome of rejection of liver transplantation in rats.

Conclusions

In summary, the blood supply of PVP microcirculation in the liver was extremely important for the transplanted liver tissue. When the blood vessels around the HBD of the rat were completely ischemic, the HBD epithelial cells became the most important target of injury, and the proliferation and changes of the HBD epithelial cells can be directly observed. VEGF could stimulate the formation and expression of new blood vessels to play a compensatory role in peripheral circulatory disorders and promote the repair of bile duct epithelial cells. In addition, the nanocarrier-mediated genes were applied

to discuss postoperative rejection. It was found that the expression of the MHC-II gene in nanocarrier CIITA-shRNA was inhibited, which interfered with the immune recognition of the graft of the recipient, thereby reducing rejection. In addition, CIITA could also participate in the regulation of the expression of a variety of antigen-presenting genes, and participate in the results of rejection of rat liver transplantation, proving that nanotechnology was worthy of further clinical promotion and application. However, the description of the experimental process was partially generalized, and the research process was time-consuming and may cause some errors. Therefore, the research process had to be improved to make the research results more accurate.

Acknowledgments

Interest conflict

The authors declare that they have no conflict of interest.

References

1. Franchitto A, Overi D, Mancinelli R, Mitterhofer AP, Muiesan P, Tinti F, Umbro I, Hubscher SG, Onori P, Gaudio E, Carpino G. Peribiliary gland damage due to liver transplantation involves peribiliary vascular plexus and vascular endothelial growth factor. Eur J Histochem 2019;63(2):3022.
2. Op den Dries S, Westerkamp AC, Karimian N, Gouw AS, Bruinsma BG, Markmann JF, Lisman T, Yeh H, Uygun K, Martins PN, Porte RJ. Injury to peribiliary glands and vascular plexus before liver transplantation predicts formation of non-anastomotic biliary strictures. J Hepatol 2014;60(6):1172-9.
3. Koda W, Harada K, Tsuneyama K, Kono N, Sasaki M, Matsui O, Nakanuma Y. Evidence of the participation of peribiliary mast cells in regulation of the peribiliary vascular plexus along the intrahepatic biliary tree. Lab Invest 2000;80(7):1007-17.
4. Huang H, Hou M, Xu J, Pang T, Duan J, Li Z, Zeng Z, Wang K. [Roles of heme oxygenase-1 promoting regeneration of peribiliary vascular plexus in bile duct ischemia/reperfusion injury]. Zhonghua Wai Ke Za Zhi 2014;52(3):193-7.
5. Uchikawa Y, Kitamura H, Miyagawa S. Portal blood flow via the peribiliary vascular plexus demonstrated by contrast-enhanced ultrasonography with Sonazoid. J Hepatobiliary Pancreat Sci 2011;18(4):615-20.
6. Kobayashi S, Kozaka K, Gabata T, Matsui O, Koda W, Okuda M, Okumura K, Sugiura T, Ogi T. Pathophysiology and Imaging Findings of Bile Duct Necrosis: A Rare but Serious Complication of Transarterial Therapy for Liver Tumors. Cancers (Basel). 2020;12(9):2596.
7. Ala A, Brown D, Khan K, Standish R, Odin JA, Fiel MI, Schiano TD, Hillan KJ, Rahman SA, Hodgson HJ, Dhillon AP. Mucosal addressin cell adhesion molecule (MAdCAM-1) expression is upregulated in the cirrhotic liver and immunolocalises to the peribiliary plexus and lymphoid aggregates. Dig Dis Sci 2013;58(9):2528-41.
8. Hennenberg M, Trebicka J, Fischer HP, Heller J, Sauerbruch T. Hepatic VASP upregulation in rats with secondary biliary cirrhosis by expression in the peribiliary vascular plexus. Microvasc Res 2009;78(2):235-40.
9. Matsui O, Miyayama S, Sanada J, Kobayashi S, Khoda W, Minami T, Kozaka K, Gabata T. Interventional oncology: new options for interstitial treatments and intravascular approaches: superselective TACE using iodized oil for HCC: rationale, technique and outcome. J Hepatobiliary Pancreat Sci 2010;17(4):407-9.
10. Chen WX, Wang F, Liu YY, Zeng QJ, Sun K, Xue X, Li X, Yang JY, An LH, Hu BH, Yang JH, Wang CS, Li ZX, Liu LY, Li Y, Zheng J, Liao FL, Han D, Fan JY, Han JY. Effect of notoginsenoside R1 on hepatic microcirculation disturbance induced by gut ischemia and reperfusion. World J Gastroenterol 2008;14(1):29-37.
11. Xiao, Z., Chen, H., Chen, H., Wu, L., Yang, G., Wu, Y. and He, N., Advanced Diagnostic Strategies for Clostridium Difficile Infection (CDI). J Biomed Nanotechnol 2019;15(6):1113-1134.
12. Chen, H., Wu, Y., Fang, Y., Liao, P., Zhao, K., Deng, Y. and He, N., Integrated and Automated, Sample-In to Result-Out, System for Nanotechnology-Based Detection of Infectious Pathogens. Nanosci Nanotechnol Lett 2018;10(1):1423–1428.
13. Liu, Y., Li, T., Ling, C., Chen, Z., Deng, Y. and He, N.,. Electrochemical sensor for Cd2+ and Pb2+ detection based on nanoporous pseudo carbon paste electrode, Chin Chem Lett 2019;30(12): 2211–2215.
14. Baudry N, Starck J, Aussel C, Lund K, Aletti M, Duranteau J, Banzet S, Lataillade JJ, Vicaut E, Peltzer J. Effect of Preconditioned Mesenchymal Stromal Cells on Early Microvascular Disturbance in a Mouse Sepsis Model. Stem Cells Dev 2019;28(24):1595-1606.
15. Li H, Lu J, Zhou X, Pan D, Guo D, Ling H, Yang H, He Y, Chen G. Quantitative Analysis of Hepatic Microcirculation in Rabbits After Liver Ischemia-Reperfusion Injury Using Contrast-Enhanced Ultrasound. Ultrasound Med Biol 2017;43(10):2469-2476.
16. Niu CY, Zhao ZG, Zhang YP, Hou YL, Li JJ, Jiang H, Zhang J. Exogenous normal lymph alleviates microcirculation disturbances and abnormal hemorheological properties in rats with disseminated intravascular coagulation. Braz J Med Biol Res 2013;46(2):138-47.
17. Friedrich S, Lüders S, Werner SG, Glimm AM,

Burmester GR, Riemekasten G, Backhaus M, Ohrndorf S. Disturbed microcirculation in the hands of patients with systemic sclerosis detected by fluorescence optical imaging: a pilot study. Arthritis Res Ther 2017;19(1):87.

18. Ito K, Kinoshita N, Koide M, Yokoi H, Irie H, Hashimoto T, Tamaki S, Nishikawa S, Azuma A, Matsubara H. [Assessment of microcirculation disturbance in patients with coronary ectasia by ATP-loading 99mTc-tetrofosmin myocardial SPECT]. Kaku Igaku 2005;42(2):79-85.

19. Khan, H., Khan, A., Liu, Y., Wang, S., Bibi, S., Xu, H., Liu, Y., Durrani, S., He, N. and Xiong, T., 2019. CRISPR-Cas13a mediated nanosystem for attomolar detection of canine parvovirus type 2. Chin Chem Lett 2019;30(12):2201-2204.

20. Lai, Y., Zhang, C., Deng, Y., Yang, G., Li, S., Tang, C. and He, N.. A novel α-fetoprotein-MIP immunosensor based on AuNPs/PTh modified glass carbon electrode. Chin Chem Lett 2019,30(1):160–162.